Stabilizing effect of elasticity is not enough to resolve discrepancies in observations concerning a moving nematic-isotropic interface

John Bechhoefer and Stephen A. Langer*
Department of Physics, Simon Fraser University, Burnaby, British Columbia, Canada V5A 1S6.
(Received 27 June 1994)

The standard theory describing the shape instability of a moving nematic-isotropic interface during the directional "solidification" of a liquid crystal disagrees with experiment by a factor of 100. We consider the stabilizing effect of the elasticity in the nematic phase and conclude that while it reduces the discrepancy, it cannot fully account for the experimental observations. The disagreement between theory and experiment remains unexplained.

PACS number(s): 64.70.Md, 81.30.Fb, 05.70.Ln, 61.30.Jf

Directional solidification, where one phase freezes at controlled velocity and temperature gradient, is important both technologically and as a setting for exploring the mechanisms of pattern formation in spatially extended nonequilibrium systems [1,2]. Although most studies have been of the solid-liquid interface, there are many advantages to experiments on the nematic-isotropic interface of liquid crystals [3–5]. The instability takes place at more convenient velocity and temperature gradient scales than in solid-liquid systems. The primary instability from a flat to a rippled interface (see Fig. 4, below) is supercritical and hence more amenable—at least in principle—to theoretical analysis than the subcritical instabilities seen in other systems. Finally, a number of interesting secondary instabilities have been discovered [3,6,7] that have stimulated much experimental and theoretical work. (For a review, see [5].)

Despite these attractive features, there have been persistent difficulties in the quantitative analysis of experimental results. There is a well-developed theory, originally by Mullins and Sekerka [8], that satisfactorily predicts instability and wavelength thresholds for solid-liquid systems [9] as well as for the discotic-isotropic interface in liquid crystals [10,11]. Yet, as we shall discuss below, the same theory gives results that are off by a factor of 100 when applied to the nematic-isotropic interface. In this article, we address two points.

(1) The discrepancy between theory and experiment is unlikely to have a "trivial" explanation (e.g., an error in the measurement of one of the material parameters that are inputs to the calculation).

(2) One plausible physical mechanism, the elasticity of the nematic phase, is too weak to resolve the discrepancy.

Because the calculation by Mullins and Sekerka is well known, we give only a bare sketch, emphasizing the physical input to the theory. (See [1,2] for more details.) We recall, first of all, the experimental setup [12]. Two ovens, separated by a small gap, are maintained at temperatures that straddle the nematic-isotropic (NI) transition. The sample is a thin (< 10 μm, typically) sandwich of glass, liquid crystal, and glass bridging the gap between the hot and cold ovens. A horizontal, linear temperature gradient G is set up in the sandwich so that the NI interface appears as a straight line somewhere in the middle of the gap. A motor then pushes the sample from the hot side to the cold side at a velocity v, forcing the interface to move at a velocity $-v$ in order to stay at the same temperature. One can easily describe the motion of the flat interface in this situation. The calculation by Mullins and Sekerka tests the linear stability of this interface to small perturbations and yields a neutral curve $G(v)$ that divides the v-G parameter plane into regions where the flat interface is or is not stable. It also gives the wavelength of the stationary cellular instability at onset.

The instability occurs because of impurities in the liquid crystal. (In a well-controlled experiment, the "impurities" would actually be the dilute limit of a known binary mixture.) The impurities have several effects.

(1) They lower the temperature of the isotropic phase and open a "freezing range" ΔT between the two phases. As a consequence, there is a jump in impurity concentration Δc at the NI interface. We can write $c_N(\zeta) = kc_I(\zeta)$, where $c_{N,I}$ is the local impurity concentration field in the N, I phases, evaluated at the interface position $z = \zeta(x,t)$, and k is the equilibrium partition coefficient, i.e., the ratio of the liquidus to solidus slopes on the phase diagram.

(2) Nonuniform concentrations of impurities lead to diffusion. The diffusion constant for impurities in the nematic phase turns out to be nearly as high as in the isotropic phase.

(3) A freezing interface will push impurity molecules to the liquid side. Conservation of impurities then requires a jump in the impurity current, i.e., in $\vec{\nabla}c$, across the interface.

The minimal model also takes into account the change due to surface tension in the equilibrium melting temperature of a curved interface, the Gibbs-Thomson effect [2]. Crudely speaking, if the nematic phase bulges out into the isotropic phase, surface tension squeezes the nematic phase, raising its internal pressure and hence lowering its equilibrium temperature via the Clausius-Clapeyron law.

One effect that we leave out is the kinetic correction

*Present address: National Institute of Standards and Technology, Gaithersburg, MD 20899-0001.

$\tilde{T}(\zeta) = \tilde{T}_0 - v/\beta$, where $T(\zeta)$ is the temperature of a moving front, T_0 is the equilibrium NI coexistence temperature, and β is the "kinetic coefficient." This term has no effect on the *thresholds* and so cannot explain the experimental observations [13]. We also make the "frozen-temperature" approximation, assuming that the local temperature is fixed by the imposed temperature gradient, and not affected by the release of latent heat. This is justified for this weakly first-order transition [14].

In the reference frame moving at a velocity v along the z axis (with the interface along the x axis), the diffusion of impurities is described by the dimensionless equations

$$\nu\nabla^2 u_N + 2\frac{\partial u_N}{\partial z} = \frac{\partial u_N}{\partial t}, \qquad z < \zeta(x,t) \tag{1a}$$

$$\nabla^2 u_I + 2\frac{\partial u_I}{\partial z} = \frac{\partial u_I}{\partial t}, \qquad z > \zeta(x,t). \tag{1b}$$

The boundary conditions at the interface are

$$u_N = k(u_I - 1), \tag{2a}$$

$$u_I = 1 - \zeta/\ell_T - d_0\kappa, \tag{2b}$$

$$(u_I - u_N)\left(2 + \frac{\partial\zeta}{\partial t}\right)\cdot\hat{\vec{n}} = (\nu\vec{\nabla}u_N - \vec{\nabla}u_I)\cdot\hat{\vec{n}}. \tag{2c}$$

The dimensionless quantities (without tildes) in Eqs. (1) and (2) are related to physical quantities (with tildes) as follows: lengths have been scaled by the diffusion length $\tilde{\ell} = 2D_I/\tilde{v}$ and times by the diffusion time $\tau = \tilde{\ell}^2/D_I$. The concentration scale is $\Delta c = [(1-k)/k]c_\infty$ where c_∞ is the average concentration of impurities in the sample as a whole. The temperature scale is $\Delta T = m\Delta c$, where m is the liquidus slope. This corresponds to the range of temperature over which there is coexistence between the nematic and isotropic phases. We then have $T = \tilde{T}/\Delta T$ and $u_{N,I} = (c_{N,I} - c_\infty)/\Delta c$. We let $\nu = D_N/D_I$ and define two more length scales: a thermal length $\tilde{\ell_T} = \Delta T/G$ and a capillary length $\tilde{d_0} = (\gamma/L)(\tilde{T}_0/\Delta T)$, where γ is the surface tension and L is the latent heat. Each of these length scales has a dimensionless counterpart $\ell_T = \tilde{\ell_T}/\tilde{\ell}$ and $d_0 = \tilde{d_0}/\tilde{\ell}$ that appears in Eqs. (2).

The ζ/ℓ_T in Eq. (2b) represents the shift in the equilibrium concentration at the interface due to the change in position (and hence temperature) of the interface. The temperature gradient enters the analysis only through this term. The Gibbs-Thomson effect enters through the $d_0\kappa$ term, with κ being the curvature of the interface.

Equations. (1) and (2) have a simple solution describing a flat interface, where $\kappa = 0$: $\zeta = 0$, $u_N = 0$ for $z < 0$, and $u_I = \exp(-2z)$ for $z > 0$. Ahead of the moving flat interface, a concentration "spike" of impurities decays exponentially over a length scale ℓ.

To test the stability of the interface, we impose a small shape perturbation $\zeta_1 = \varepsilon\exp(\omega t + iqx) +$ c.c. and linearize the equations of motion with respect to ε. The result is an implicit relation for the growth rate ω of a perturbation of wave number q. In the special case of the symmetric model ($\nu = k = 1$), $\Delta T > 0$, one finds [15]

$$\omega = -2 + 2(1 - \ell_T^{-1} - d_0q^2)(1 + q^2 + \omega)^{1/2}. \tag{3}$$

The dispersion relation for the more general case (ν and k different from 1) is given in the Appendix. We emphasize that for ν and $k \approx 1$, the dispersion relation does not qualitatively change. The neutral curve and onset wave number q^* are obtained by solving (numerically) the simultaneous equations $\omega(q^*) = \partial\omega(q^*)/\partial q = 0$. Sample curves are shown in Figs. 1 and 2. Note that there is a maximum freezing velocity $v_{\max}$ and temperature gradient $G_{\max}$ beyond which the interface is always stable. There is also a maximum wave number $q_{\max}$ (or minimum wavelength). For the symmetric model, these quantities are given in dimensional units by

$$v_{\max} = \frac{D}{\tilde{d_0}}, \qquad G_{\max} \approx \frac{\Delta T}{\tilde{d_0}}, \qquad q_{\max} = \frac{1}{\tilde{d_0}}. \tag{4}$$

In the more general case (ν and $k \neq 1$), the scalings are still valid, although the coefficients depend on ν and k. As long as these two parameters are close to 1 (and they are in our case), the coefficients will also be of order 1.

The first experiments on directional solidification of the NI interface by Oswald *et al.* [16,12] were complicated by the presence of solutal convection. The added impurity, C_2Cl_6, had a density that was about twice that of the host liquid crystal, 8CB (4′-*n*-octylcyanobiphenyl). The concentration gradient in front of the NI interface led to a backroll where the heavy impurities sank, bringing in purer liquid to the interface and raising the effective diffusion constant. By making the sample thinner than about 5 μm, the effect disappeared, but no detailed comparison was made with the Mullins-Sekerka theory for these thin samples.

Recently, Figueiredo *et al.* [17] redid the experiment using 8CB with absorbed water as the impurity. Because

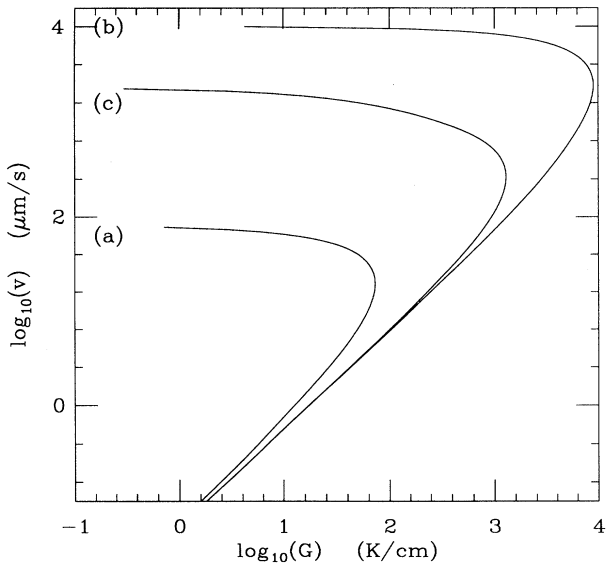

FIG. 1. Marginal-stability curves dividing the velocity-temperature gradient parameter plane into stable and unstable regions for fixed overall impurity concentration. (a) Curve deduced from the measurements by Figueiredo *et al.* (b) Curve deduced using the known value of γ and L. (c) Curve deduced using the known parameter values and adding elastic effects.

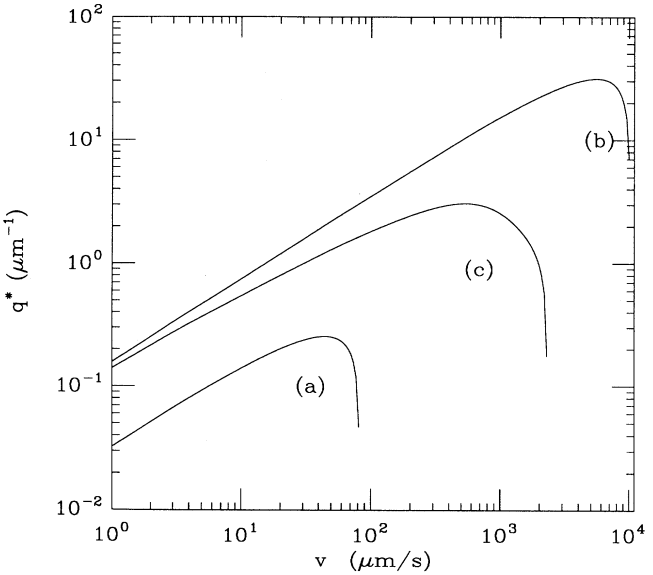

FIG. 2. Onset wave number vs freezing velocity for fixed overall impurity concentration. (a) Curve deduced from the measurements by Figueiredo *et al.* (b) Curve deduced using the known values of γ and L. (c) Curve deduced using the known parameter values and adding elastic effects.

the sample thickness was 3.5 μm and because $\rho_{H_2O} = 1.00$ gm/cm^3 nearly matches $\rho_{8CB} = 0.97$ gm/cm^3, solutal convection was negligible. (Thermal convection can also be shown to be negligible in such thin samples [12].) They inferred the various material parameters, including γ/L, by fitting their data for the growth rates ω and onset wave numbers q^* to the standard Mullins-Sekerka theory. All of the values that they deduce are reasonable except for the ratio γ/L, whose value is 100 times larger than the value obtained by independent measurements. Furthermore, the Mullins-Sekerka theory, using either the parameters inferred by Figueiredo *et al.* or the parameters deduced by different types of experimental measurements of γ and L, predicts values for v_{max}, G_{max}, and q_{max} that are each 100 times larger than the values measured in the experiment. (See Table I.)

Our first point is that with the exception of the ratio γ/L, any errors in the parameter values are unlikely to explain the discrepancy between the predicted and observed instability scales. We consider each parameter in turn.

c_∞: The value of 0.14 mol % matches the equilibrium concentration of water in 8CB (0.15 mol %) specified by the manufacturer, BDH. Further, the sample would have to be much *purer* to bring the numbers into even approximate agreement.

m and k: Ghodbane and Martire [18] measured the liquidus slope and partition coefficient for 20 different impurities in 8CB. In all cases, they found $0.8 < m < 1.8$ °C/mol% and $0.72 < k < 0.92$. The values in Table I fall within this range.

ΔT: As a final check, $\Delta T = mc_\infty(1-k)/k$ was measured directly in our laboratory on a similar 8CB sample. We found $\Delta T = 0.21$ °C, which is roughly consistent with the data of Figueiredo *et al.* To get approximate agreement would require $\Delta T \approx 10^{-3}$ °C.

TABLE I. Parameter values for the directional solidification of 8CB used to compute curve (b) in Figs. 1 and 2 (data from [12,17]). The parameters G^*, v^*, and q^* are typical destabilization values found in [17].

c_∞	0.14 ± 0.02	(mol %)
m	1.35	(°C/mol %)
k	0.740 ± 0.004	
D_I	6.7 $\times 10^{-7}$	(cm^2/sec)
ν	0.5	
γ	0.95 ± 0.4 $\times 10^{-2}$	(erg/cm^2)
L	2.05 ± 0.02 $\times 10^7$	(erg/cm^3)
γ/L	0.047	(Å)
G^*	43	(°C/cm)
v^*	10	(μm/sec)
q^*	0.1	(μm^{-1})

D_N and D_I: Independently measured values of D_I for self-diffusion of 8CB and of dye molecules give 4–5$\times 10^{-7}$ cm^2/sec [12]. The diffusion constant of water should be a little higher. Diffusion in the nematic phase is anisotropic: small molecules diffuse faster (usually by about 25%) along the director of the nematic phase than across it. Because the samples in the experiments are homeotropic (i.e., the nematic molecules are constrained to be perpendicular to the glass plates at the boundaries), one is tempted to use $D_{N_\perp}$ which leads one to expect $\nu \approx 0.5$; however, the scales v_{max}, G_{max}, and q_{max} are rather insensitive to the precise choice of ν. For example, they vary by less than 20% as ν changes from 0.5 to 1.0.

We note in passing that the control parameters v, G, and q are all measured directly in the experiment to an accuracy that is easily better than 5%. They cannot explain the error.

The final two parameters are the surface tension γ and the latent heat L. The experiment is sensitive to their ratio through the Gibbs-Thomson effect, and they come into the theory via the dimensionless capillary length d_0. Figueiredo *et al.* conclude that the ratio γ/L should be 6 Å. Such a value is in itself unremarkable, for it closely matches that deduced in solid-liquid [9] and discotic-isotropic [10,11] experiments.

However, independent measurements of γ and L indicate that their ratio is approximately 0.05 Å. (See Table I.) The latent heat of 8CB has been measured by adiabatic scanning calorimetry [19] and confirmed by careful differential scanning calorimetry measurements [20]. Likewise, the surface tension of the NI interface is consistently of order 10^{-2} erg/cm^2 and has been measured using light scattering [21], interface reflectivity [22], sessile drops [23], and electric fields [24,25]. Perhaps the most convincing measurement for our purposes is that by Armitage and Price [26], who showed that embedding the liquid crystal in a porous medium with 100 Å pores depressed the NI transition temperature by only 0.1 °C. This gives the ratio γ/L directly: $R(\Delta T/T_0) =$ 100 Å (0.1/400) $\approx$ 0.025 Å.

Why might γ/L be so small? Ordinarily, one expects γ/L to be approximately the bare correlation length, ξ_0.

This length is usually a few angstroms (it is also close to the thickness of the interface) and explains why most directional solidification experiments deduce similar values for γ/L. The NI system has a much smaller value of γ/L because the transition is nearly second order, and critical effects are important [28]. Approaching a critical point, both γ and L vanish and one can show that $\gamma/L \approx \xi_0(\xi_0/\xi) \to 0$ [12].

Thus we conclude that the surprisingly small value of 0.05 Å is real, although it completely disagrees with the results of the solidification experiment. Nonetheless, of all the material parameters, we focus on this one for two reasons.

(1) The three quantities $v_{\max}$, $G_{\max}$, and $q_{\max}$ are all off by a factor of 100. The only parameter that affects all three parameters linearly is γ/L. For example, in Eq. (4), we see that the diffusion constant affects $v_{\max}$ but not $G_{\max}$ or $q_{\max}$. Also ΔT (and hence c_∞) enters linearly in $v_{\max}$ and $q_{\max}$ but quadratically in $G_{\max}$.

(2) The mathematical role of γ/L is to provide a cutoff length that stabilizes against small perturbations. If the surface tension is so small that the cutoff length is less than a molecular size, then it is reasonable to look for another stabilizing force. An obvious candidate is the elasticity of the nematic phase. Molecules are known to lie at a preferred angle at the NI interface. If this angle is maintained while the interface is deformed, the nematic will be stressed elastically. We now examine the consequences [27].

We shall simplify somewhat the physics to make the calculation tractable while still illustrating the orders of magnitude that arise. We constrain the nematic director to lie in the xz plane, and continue to neglect three-dimensional effects (see below, however). The local molecular orientation is then characterized by the angle $\varphi(x,z,t)$, where we define $\varphi = 0$ to be along the z axis and $\varphi = \pi/2$ to be along the $+x$ axis. We assume that there is never any fluid flow in the nematic; that is, our nematic "hydrodynamics" includes only the dynamic reorientation of the director. Because the samples are thin (3.5 μm), this is reasonable. We assume strong anchoring, i.e., we assume that the director molecules always maintain their preferred orientation with respect to the interface, whatever the interface deformation. (In fact, this is not true experimentally, but making this assumption *maximizes* the elastic effect.) Finally, we use the "one-constant" elastic-energy approximation, in which bend, splay, and twist deformations all cost equal energy. In this approximation, when the director is constrained to lie in the plane, the elastic energy per unit height takes the form [28]

$$E_{\rm el} = \frac{1}{2}K\int dx\,dz\;|\nabla\varphi|^2\,. \tag{5}$$

K is the Frank elastic constant ($\approx 10^{-6}$ dyn). The director orientation relaxes with a rotational viscosity γ_1 (0.1 P), leading to an equation of motion [29] $\gamma_1\partial\varphi/\partial t = -\delta E_{\rm el}/\delta\varphi$, which in the moving frame becomes

$$\frac{\partial\varphi}{\partial\tilde{t}} = \frac{K}{\gamma_1}\tilde{\nabla}^2\varphi + \tilde{v}\frac{\partial\varphi}{\partial\tilde{z}}. \tag{6}$$

This must be solved with the assumed strong anchoring boundary conditions. Rescaling Eq. (6) introduces the dimensionless parameter $\eta = K/(\gamma_1 D_I) \approx 20$, which suggests that elastic coupling can be important.

Setting $\varphi \equiv 0$ leaves the previously obtained flat-interface solution unchanged. Perturbing about this solution, $\varphi = \varepsilon\exp(Qz + \omega t + iqx) + \text{c.c.}$, and substituting into the dimensionless form of (6) gives an inverse elastic decay length $Q = [\sqrt{1+\eta\omega+\eta^2q^2} - 1]/\eta$. Usually, $q \gg 1$, so that $Q \approx q$ — elastic deformations are expected to penetrate about one wavelength into the bulk nematic.

Next, we compute the generalization of the Gibbs-Thomson correction: elastic deformations raise the free energy of the nematic phase and, by an analog of the Clausius-Clapeyron law, lower its coexistence temperature with the isotropic phase. Let h be the thickness of the sample, A the area of the nematic phase, and $L_{\rm int}$ the length of the nematic-isotropic interface. Then the energy E is

$$\frac{1}{h}E = \Delta pA + \gamma L_{\rm int} + \frac{1}{2}K\int dx\int_{-\infty}^{0} dz\,|\nabla\varphi|^2. \tag{7}$$

Since $\varphi(x,z)$ depends on $\zeta(x)$, E is a functional of ζ. In equilibrium

$$\frac{\delta E}{\delta\zeta} = 0. \tag{8}$$

Substituting the first two terms on the right-hand side of (7) into (8), and using

$$\frac{\delta A}{\delta\zeta} = \frac{\delta}{\delta\zeta}\int dx\zeta(x) = 1 \tag{9}$$

and

$$\frac{\delta L_{\rm int}}{\delta\zeta} = \frac{\delta}{\delta\zeta}\int dx\sqrt{1+\zeta'^2} = -\frac{\zeta''}{(1+\zeta'^2)^{3/2}} \equiv -\kappa \approx -\frac{\partial^2\zeta}{\partial x^2} \tag{10}$$

yields the usual Gibbs-Thomson relation, when the Δp is related to Δc through the Clausius-Clapeyron law.

In the third term of Eq. (7), let $\varphi(x,z) = \varphi_0(x)\exp(Qz)$, where the inverse decay length Q is given above and where the boundary condition (strong anchoring) requires

$$\varphi_0(x) = \partial\zeta/\partial x + o(\zeta^2), \tag{11}$$

up to an unimportant constant. Then

$$\int dx\int_{-\infty}^{0} dz\,|\nabla\varphi|^2 = \int dx\int_{-\infty}^{0} dz\,(\partial_x\varphi_0 + Q\varphi_0)^2 e^{2Qz} \tag{12}$$

$$= \int dx\left\{\frac{1}{2Q}(\partial_x\varphi_0)^2 + \frac{1}{2}Q\varphi_0^2\right\} + \text{boundary terms} \tag{13}$$

$$\approx \int dx\left\{\frac{1}{2Q}\left(\frac{\partial^2\zeta}{\partial x^2}\right)^2 + \frac{1}{2}Q\left(\frac{\partial\zeta}{\partial x}\right)^2\right\}. \tag{14}$$

The first term in the integrand looks like a rigidity, as in the Helfrich model for membranes [30]. Taking the functional derivative,

$$\frac{\delta}{\delta\zeta}\int dx\,dz\,|\nabla\varphi|^2 = \frac{1}{Q}\frac{\partial^4\zeta}{\partial x^4} - Q\frac{\partial^2\zeta}{\partial x^2}. \tag{15}$$

Now Eq. (8) becomes

$$0 = \Delta p - \gamma\kappa + \frac{1}{2}\frac{K}{Q}\frac{\partial^4\zeta}{\partial x^4} - \frac{1}{2}KQ\kappa. \tag{16}$$

Scaling this equation,

$$\Delta p' \equiv \frac{d_0}{\gamma}\Delta p = d_0\kappa - \frac{1}{2}\ell_E^2\left(\frac{1}{Q}\frac{\partial^4\zeta}{\partial x^4} - Q\kappa\right), \tag{17}$$

and perturbing ζ with a sinusoid of wave number q, we see that the term d_0q^2 in the scaled dispersion relation (3) should be replaced by $d_0q^2 + (1/2)\ell_E^2(q^4/Q + Qq^2)$, where the elastic length $\ell_E^2 = (K/L)(\tilde{T}_0/\Delta T)/\ell^2$. The full dispersion relation becomes (again for $\nu = k = 1$, although our numerical work was for the general case; see the Appendix)

$$\omega(q) = -2 + \left[\left(1 - \ell_T^{-1}\right) - d_0q^2 - \frac{1}{2}\ell_E^2\left(Qq^2 + \frac{q^4}{Q}\right)\right] \times\sqrt{1+\omega+q^2}. \tag{18}$$

The results of the calculation are shown in Figs. 1 and 2. In each of these figures, curve (a) uses the parameters deduced by Figueiredo *et al.* from the free fit to their data. Curve (b) substitutes the known value of γ/L, illustrating the 100-fold discrepancy with curve (a). Curve (c) uses the same parameters as in (b) but also includes elastic effects.

Although elasticity reduces the discrepancy between theory and experiment, it still leaves a wide gap to be explained. Moreover, we have probably overestimated the importance of elastic effects in our own calculation. As we have mentioned above, the anchoring at the interface is not strong, contrary to our assumption in (11). Faetti and Palleschi have measured the surface tension, anchoring angle, and anchoring strength of the NI interface of 8CB [22]. By measuring the interface reflectivity in the presence of a magnetic field, they deduce

$$\gamma = \gamma_0 + A(\varphi - \varphi_0)^2, \tag{19}$$

with γ_0 given in Table I, $\phi_0 = 48.5 \pm 6°$, and $A = 8.5 \pm 2.1 \times 10^{-4}$ erg/cm^2 the anchoring strength; i.e., $A/\gamma_0 = 0.09 \ll 1$. These numbers are also consistent with a similar study using electric-field deformation [31]. Thus any elastic distortions in the nematic will be largely relaxed by changing the value of φ at the NI interface.

One might wonder whether the three-dimensional structure of the director field near the interface is relevant. As argued on the basis of polarizing microscope observations in previous work [16,12], the interface and surrounding director field are as depicted in Fig. 3. It is easy to rule out the effects of the nonsingular distortions. Imposing representative director configurations with nonsingular variations over the sample thickness leads to $O(1)$ changes in the elastic free energy. The effect of the disclination line shown in Fig. 3 is less clear. The experimental evidence, however, argues against its relevance. When the interface is driven rapidly enough, the disclination line detaches [16,32,33]. Because the defect line moves with a maximum velocity $v_{\rm line} \approx K/(\gamma_1 h)$, it cannot catch up to the front if $v > v_{\rm line}$. The defect line detaches hysteretically; the interface must go much faster

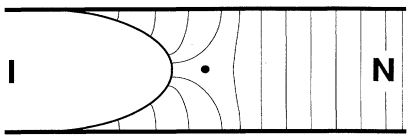

FIG. 3. Side view of the meniscus between the nematic and isotropic phases. The orientations of nematic molecules in this homeotropically anchored sample are shown. Note the disclination line just behind the interface. (The line is perpendicular to the plane of the figure.)

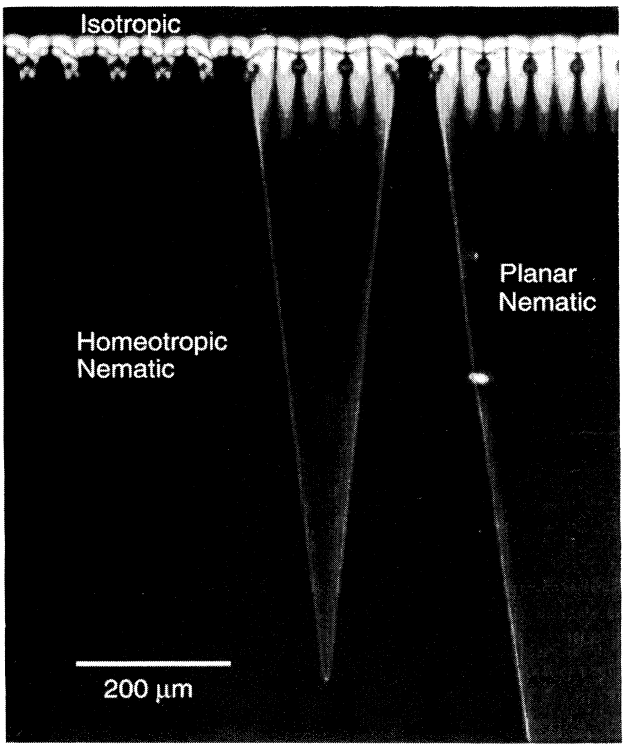

FIG. 4. Triangle domains viewed between crossed polarizers. The large triangles are regions of nematic oriented in the plane of the sample plates, while the surrounding material is homeotropic (perpendicular to the plates). The baroque architecture of the NI interface is due to the structure of the meniscus. Within the triangles, the defect line is detached, and our analysis (see text) applies. Note that in these regions the nematic director field is distorted to a distance comparable to the wavelength, and that the wavelength of the instability is slightly increased.

than $v_{\rm line}$ to detach the defect, probably because of extra pinning forces localized to the interface. The result, illustrated in Fig. 4, is that regions where the defect line is or is not attached may coexist. As Fig. 4 shows, the presence or absence of the defect line has little effect on the wavelength of the instability. (More careful observations suggest that the wavelength increases about 10% when the line is detached [32,33].) We have also made observations on planar and randomly oriented samples (using untreated glass plates for the latter). In each of these cases, the wavelengths and thresholds do not vary dramatically despite the variety of directory configurations. Therefore, since the defect line strongly affects the three-dimensional (3D) structure of the director field, and since its presence does not significantly affect the wavelength of the instability, we conclude that the 3D structure of the director field does not strongly alter our results.

Another effect that we have not considered is the three-dimensional shape of the interface. Because the zero-order solution is curved in the vertical direction, the linear stability analysis is modified. This has been discussed for the symmetric model by Caroli *et al.* [34], who conclude that the velocity thresholds are indeed depressed. They, however, assumed that the contact angle between the meniscus and the glass plates was close to 90°, which is not true for the NI interface. More experimental and theoretical work is required to assess the relevance of these thickness effects.

While calculating the elastic effects discussed above, we learned that Misbah and Valance [35,36] had also considered effects of elasticity on the interface instability; however, they focus on the coupling between the director field and the anisotropic diffusion in the nematic. They did not evaluate the specific coupling that we discuss here.

We have reviewed the theories and measurements of the shape instability of a moving nematic-isotropic interface. The simplest theories yield numbers that are 100 times larger than the observed values, a discrepancy that is too large to explain away by inaccurate material parameter measurements. We then considered the effects of the nematic's elasticity. The evidence from our calculation and from the experiments themselves is that elastic effects are noticeable but small. Some other physical mechanism seems responsible for imposing the inferred cutoff length of 6 Å, but the source of this stabilization remains a mystery.

This work was supported by NSERC. J.B. is supported by the Alfred P. Sloan Foundation. We are grateful to Chaouqi Misbah for correspondence and for making results available to us in advance of publication. We thank Nancy Tamblyn and Angelo Miele for measuring the value of ΔT.

APPENDIX

Here, we give the full dispersion relation that we used in our numerical calculations. We emphasize that for the case of the nematic-isotropic interface, where the partition coefficient k and the ratio of diffusion constants ν is roughly 1, the special case of the dispersion relation given in the text has all the qualitative features of the algebraically more complicated exact relation. For the dispersion relation, we find

$$\omega = -2 + (1-k)(\ell_T^{-1} + f) + (2 - \ell_T^{-1} - f)\sqrt{1 + q^2 + \omega} - k(\ell_T^{-1} + f)\sqrt{1 + \nu^2 q^2 + \nu\omega}, \tag{A1}$$

where

$$f(q,\omega) = d_0 q^2 + \frac{1}{2}\ell_E^2 (Q q^2 + q^4/Q). \tag{A2}$$

Note again that elastic effects enter only through the ℓ_E term.

[1] J. S. Langer, Rev. Mod. Phys. **52**, 1 (1980).
[2] B. Caroli, C. Caroli, and B. Roulet, in *Solids Far from Equilibrium,* edited by C. Godrèche (Cambridge University Press, Cambridge, England, 1992), p. 155.
[3] J.-M. Flesselles, A. J. Simon, and A. J. Libchaber, Adv. Phys. **40**, 1 (1991).
[4] P. Oswald, J. Bechhoefer, and F. Melo, MRS Bull. **16**, 38 (1991).
[5] J. Bechhoefer, in *Pattern Formation in Liquid Crystals*, edited by L. Kramer and A. Buka (Springer-Verlag Berlin, in press).
[6] A. J. Simon, J. Bechhoefer, and A. Libchaber, Phys. Rev. Lett. **61**, 2574 (1988).
[7] A. J. Simon and A. Libchaber, Phys. Rev. A **41**, 7090 (1990).
[8] W. W. Mullins and R. F. Sekerka, J. Appl. Phys. **35**, 444 (1964).
[9] S. de Cheveigné *et al.*, J. Cryst. Growth **92**, 616 (1988).
[10] P. Oswald, J. Phys. (Paris) **49**, 1083 (1988).
[11] P. Oswald, J. Phys. (Paris) **49**, 2119 (1988).
[12] J. Bechhoefer, A. J. Simon, and A. Libchaber, Phys Rev. A **40**, 2042 (1989)
[13] The kinetic correction adds a term proportional to ω to the dispersion relation (3). Because the threshold is evaluated at $\omega = 0$, it is unchanged. The growth rate measured by Figueiredo *et al.* would be changed, but that would not explain the discrepancy between onset threshold and onset wave number that they observed. See R. G. Seidensticker, in *Crystal Growth*, edited by H. S. Peiser (Pergamon, Oxford, 1967), p. 733. See also C. Misbah, H. Müller-Krumbhaar, and D. E. Temkin, J. Phys. I **1**, 585 (1991).
[14] J.-C. Géminard, Ph.D. thesis, Université Claude Bernard–Lyon I, 1993, pp. 14–16, shows that the effects of the latent heat are negligible if $-(Lhv/\kappa_g \Delta T)\ln(vhc_g/8\pi\kappa_g) \ll 1$, where κ_g and c_g are the thermal conductivity and heat capacity of the glass plates. (The remaining variables are defined in the text above.) We estimate this quantity to be $\approx 10^{-2}$ in our case.

[15] We actually used the general case $\nu < 1$, $k < 1$ in our numerical calculations. See the Appendix, as well as [35] and B. Caroli, C. Caroli, and B. Roulet, J. Phys. (Paris) **43**, 1767 (1982).
[16] P. Oswald, J. Bechhoefer, and A. Libchaber, Phys. Rev. Lett. **58**, 2318 (1987).
[17] J. M. A. Figueiredo, M. B. L. Santos, L. O. Ladeira, and O. N. Mesquita, Phys. Rev. Lett. **71**, 4397 (1993).
[18] S. Ghodbane and D. E. Martire, J. Phys. Chem. **91**, 6410 (1987).
[19] H. Marynissen, J. Thoen, and W. van Kael, Mol. Cryst. Liq. Cryst. **97**, 149 (1983).
[20] B. R. Ratna and S. Chandrasekhar, Mol. Cryst. Liq. Cryst. **162B**, 157 (1988).
[21] D. Langevin and M. A. Bouchiat, Mol. Cryst. Liq. Cryst. **22**, 317 (1973).
[22] S. Faetti and V. Palleschi, Phys. Rev. A **30**, 3241 (1984).
[23] R. Williams, Mol. Cryst. Liq. Cryst. **35**, 349 (1973).
[24] H. Yokoyama, S. Kobayashi, and H. Kamei, Mol. Cryst. Liq. Cryst. **129**, 109 (1985).
[25] C. S. Park, N. A. Clark, and R. D. Noble, Phys. Rev. Lett. **72**, 1838 (1994).
[26] D. Armitage and F. P. Price, Chem. Phys. Lett. **44**, 305 (1976).
[27] The effects of elasticity of the solid phase have been examined for the Mullins-Sekerka instability of a solid-liquid interface. We note that both the form of the elastic energy and its magnitude relative to other energies in the problem are very different so that those calculations are not directly relevant to our case. See B. Caroli, C. Caroli, B. Roulet, and P. W. Voorhees, Acta Metall. **37**, 330 (1987); and B. J. Spencer, P. W. Voorhees, S. H. Davis, and G. B. McFadden, Acta Metall. Mater. **40**, 1599 (1992) for treatment of the solid-liquid case.
[28] P. G. de Gennes and J. Prost, *The Physics of Liquid Crystals,* 2nd ed. (Oxford University, New York, 1994).
[29] S. Chandrasekhar, *Liquid Crystals,* 2nd ed. (Cambridge University, Cambridge, England, 1992), p. 161.
[30] W. Helfrich, Z. Naturforsch. **28**, 6693 (1973).
[31] H. Yokoyama, S. Koyayashi, and H. Kamei, Mol. Cryst. Liq. Cryst. **107**, 311 (1984).
[32] J. Bechhoefer, Ph. D. thesis, The University of Chicago, 1988.
[33] P. Oswald, J. Phys. II **1**, 571 (1991).
[34] B. Caroli, C. Caroli, and B. Roulet, J. Cryst. Growth **76**, 31 (1986).
[35] A. Valance, Thèse de Doctorat, Université de Paris 7, 1993.
[36] C. Misbah and A. Valance (unpublished)

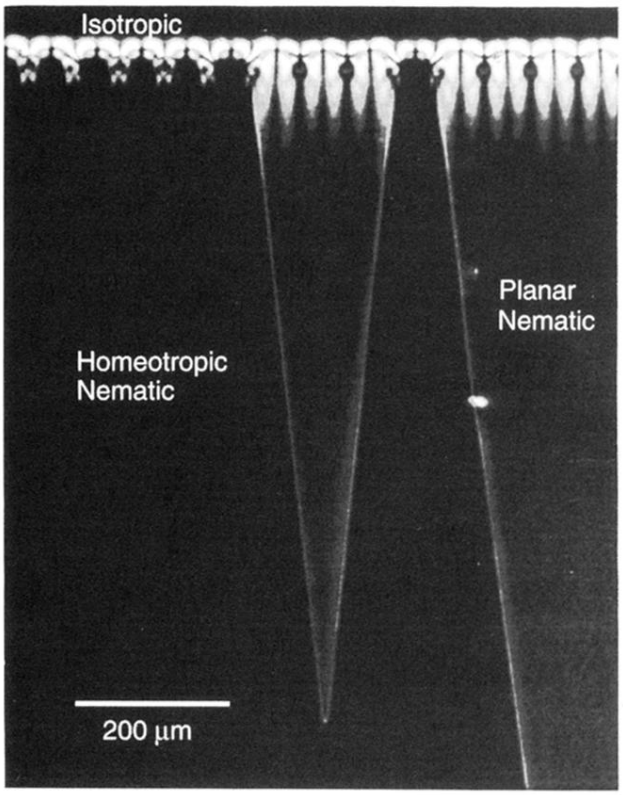

FIG. 4. Triangle domains viewed between crossed polarizers. The large triangles are regions of nematic oriented in the plane of the sample plates, while the surrounding material is homeotropic (perpendicular to the plates). The baroque architecture of the NI interface is due to the structure of the meniscus. Within the triangles, the defect line is detached, and our analysis (see text) applies. Note that in these regions the nematic director field is distorted to a distance comparable to the wavelength, and that the wavelength of the instability is slightly increased.